

Effect of tool offset on weld characteristics during dissimilar micro-friction stir welding of AA 6061-T6 and ALCLAD 2024-T3

Mayank Verma, Probir Saha*

Indian Institute of Technology Patna, Bihta, Patna, Bihar, India

Presented in International Conference on Precision, Micro, Meso and Nano Engineering (COPEN - 12: 2022)

December 8th - 10th, 2022 IIT Kanpur, India

ABSTRACT

KEYWORDS

Dissimilar Micro-Friction Stir Welding (μ FSW), Tool Offset, Material Intermixing, Ultra-Thin Sheets, Fractography.

A sound dissimilar welded thin sheet joint is required in various engineering applications to meet the demand for miniaturized products. The major concern is rapid heat dissipation which causes improper material intermixing and poor weld performance. Tool offset can resolve this issue. So, in the present work, 0.5 mm thick AA 6061-T6 and ALCLAD 2024-T3 were welded. The tool was offset on the 2024 (high-strength) side to ensure appropriate heat distribution and maximize the involvement of 2024 in weld zone. The degree of material intermixing is defined based on the number of intercalated layers and thickness of the layer of 2024 in stir zone (SZ). The highest weld efficiency of 77.97% was obtained at a tool offset distance of 0.6 mm due to mechanical interlocking produced by more intercalated layers. Moreover, the weld fractures from the heat-affected zone of 6061, unlike other cases where it fractures from the SZ.

1. Introduction

Friction stir welding (FSW) was primarily used to join aluminum alloys but was later expanded to join dissimilar materials due to the advantages obtained from the solid-state joining technique (Threadgill et al., 2009). To join thin dissimilar sheets (thickness $\leq 1000 \mu\text{m}$) and to meet the growing demand for miniaturized parts, a new variant of FSW was developed, known as micro-friction stir welding (μ FSW) (Teh et al., 2011). The primary concern associated with joining dissimilar materials is meeting the demand of the two different materials having different softening characteristics placed on either side of the weld centerline. This problem gets amplified in the joining of ultra-thin sheets due to a relatively lower heat sources and an increased rate of heat dissipation from the weld zone (Verma et al., 2021). As a result, improper material intermixing occurs, eventually leading to the poor mechanical performance of the joint.

Tool offset can be one of the techniques to fulfill the requirement of different aluminum alloys placed on either side of the weld centerline to

obtain superior weld strength (Kumar & Kailas, 2010). This technique has been applied for the joining of thicker materials. In one such work where a 4.7 mm thick AA 2014 and AA 6061 were joined, it was concluded that a lower welding temperature was obtained, which limits the growth of hardening precipitates on the 6061 side when the tool was offset on the 2014 side, leading to increased joint strength (Jonckheere et al., 2012). In another work, fatigue strength increased when the tool was offset on the 2024 side during the joining of 4 mm thick AA 2024 and AA 7075 (Cavaliere & Panella, 2008). In another study, Cole et al. (2014) carried out dissimilar FSW of AA 6061-T6 and AA 7075-T6, both of thickness 4.76 mm. In this work they deduced that the highest joint was achieved when the tool was offset on a higher hot-strength side (7075).

The literature revealed the importance of the tool offset during dissimilar FSW of thicker sheets ($> 1 \text{ mm}$). Moreover, there was no literature available where the concept of tool offset was applied to the joining of thin dissimilar aluminum alloys ($< 1 \text{ mm}$), except the one where a 1 mm thick AA 6061-T6 and T2 pure copper were joined (Mao et al., 2020). However, considering the relatively higher rate of heat dissipation in thinner sheets, tool offset will be an important

*Corresponding author E-mail: psaha@iitp.ac.in

aspect of achieving better material intermixing by providing the right amount of heat distribution to the two different alloys. Therefore, in the present work, 0.5 mm thin AA 6061-T6 and ALCLAD 2024-T3 were carried out, and the tool was offset towards 2024 (high-strength alloy) at different distances. Further, the effect of tool offset on the weld characteristics, i.e., material intermixing and mechanical performance was carried out.

2. Materials and Methods

ALCLAD 2024-T3 (high-strength aerospace grade) and AA 6061-T6 (medium-strength), both 0.5 mm thick, were considered as the workpiece materials. The difference in their solidus temperature is about 80°C. There was a cladding of pure aluminum (ALCLAD) on the top and bottom surface of 2024, whose thickness was about 0.025 mm (~ 5% of total sheet thickness). The presence of ALCLAD layer increases the corrosion resistance property of the material. The detailed dimensions of the triple-spiral micro-grooves featured tool used for the welding are shown in Fig. 1a. The micro-groove had a circular cross-section. The tool was manufactured to the required dimensions using a micro-machining center (make: MIKROTOOLS, model: DT-110), where micro-turning and micro-milling operations were performed. The dissimilar μ FSW experiment was carried out on a CNC milling machine (make: MTAB, model: FLEXMILL) using an in-house developed fixture (Ahmed & Saha, 2018).

The workpiece was prepared to the required dimensions using a wire-EDM machine (make: ELECTRONICA, model: SPRINTCUT). These workpieces were arranged in a butt configuration, with 6061 positioned on the advancing side (AS), and that 2024 on the retreating side (RS). Because of the higher localized temperature on AS, the material with higher solidus temperature was positioning on this side (Cole et al., 2014). The tool was offset towards the 2024 side (RS) to increase the involvement of high-strength material in the weld zone by increasing the heat input on this side (see Fig. 1b). Two different values (0.4 mm and 0.6 mm) of offset were selected, and the maximum offset value was kept at less than 60% of the pin tip radius (i.e., 1.1 mm). The values were selected on the basis of literature and the fixturing constraint related to the FSW of thin sheets (Ahmed & Saha, 2018). So, in total, there were three cases: one weld at the faying surface or zero offset (0-off) and the other at different

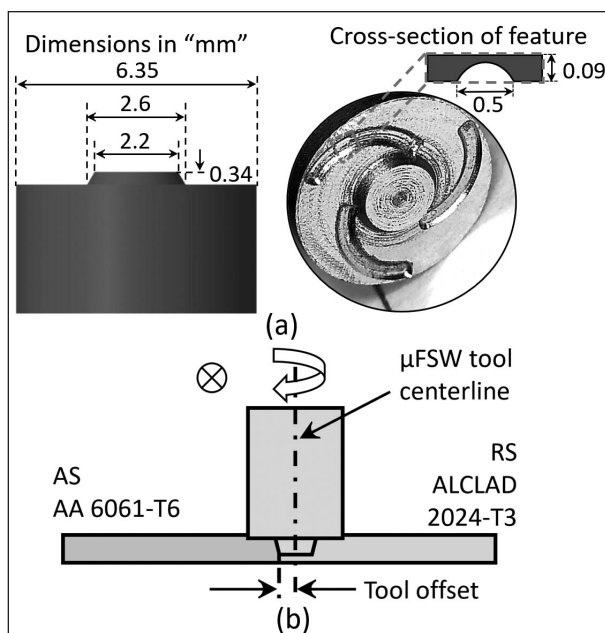


Fig. 1. (a) Detailed dimensions of the μ FSW featured tool, and (b) schematic illustrating tool offset on ALCLAD 2024-T3 side.

offset positions (0.4-off and 0.6-off). The tool rotational speed, travel speed and tilt angle were 2000 rpm, 175 mm/min, and 1°, respectively, which were considered based on the pilot experiment. Moreover, the total plunge depth of 0.45 mm were considered.

For post-weld analysis, subsize tensile (ASTM-E8 standard) samples perpendicular to the welding direction and metallographic samples were prepared using wire-EDM. The metallographic samples were systematically prepared and chemically etched with Keller's reagent (2.5 ml HNO₃, 1.5 ml HCl, 1 ml HF and 95 ml H₂O). The samples were then observed using an optical microscope (make: ZEISS, model: ImagerM2M) to analyze the material flow and its intermixing. The uniaxial tensile tests were carried out on a universal testing machine (UTM) (make: BISS, model: Nanobiss) at a cross-head speed of 0.25 mm/min or strain rate of $1.6 \times 10^{-4} \text{ s}^{-1}$. The fracture morphology was inspected using field emission scanning electron microscopy (FE-SEM) (make: ZEISS, model: GeminiSEM 500), following the tensile test.

3. Results and Discussion

3.1. Macrograph analysis

The macrographs of all three cases (0-off, 0.4-off, and 0.6-off) and their magnified views are shown

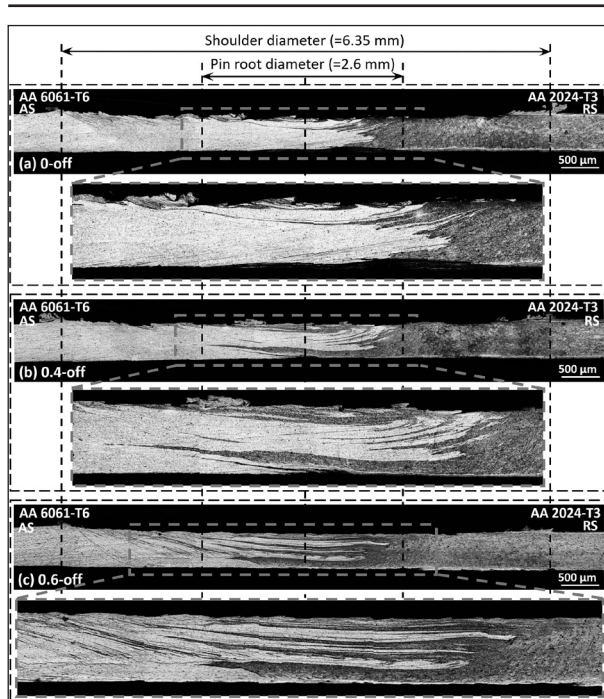


Fig. 2. Macrographs depicting the weld’s cross-section of (a) 0-off, (b) 0.4-off, and (c) 0.6-off with the respective magnified view of the center region.

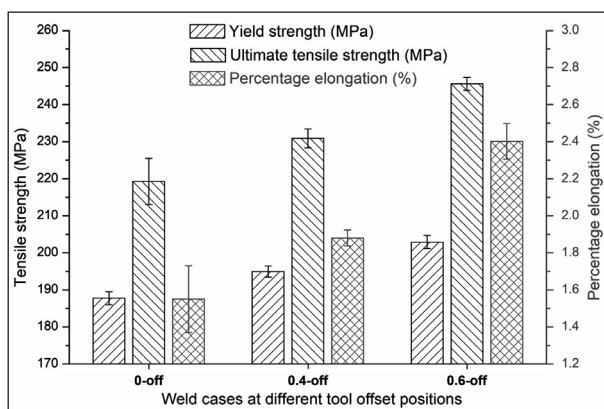


Fig. 3. Comparative bar plot of the tensile properties obtained in different cases.

in Fig. 2. The shoulder diameter and the pin root diameter has been marked in the same image to understand the interaction of tool with the workpiece. After the etching of the metallographic samples with Keller’s reagent, the etch contrast was produced due to the difference in the etching response of two different alloys. The AA 6061 appears lighter, whereas the AA 2024 appears darker. The contrast produced due to etching was used for the visualization of the material flow and to study the extent of material intermixing in the weld zone. The macrographs clearly showed the effect of different tool offset positions on the weld formation. Moreover, it can be said that there were no visible defects such as tunnel defect, cavities, lack of penetration, and others.

A common observation is that layer-wise mixing of both materials occurred in all three cases. However, the extent or the degree of material intermixing was different in all cases. In the present work, the extent of material intermixing was defined on the basis of – (i) the number of intercalated layers observed in the stir zone (SZ) and (ii) thickness of the layer of AA 2024 material in the SZ. The involvement of AA 2024 was focused on because, from the literature, it was discovered that the presence of higher-strength material in the SZ results in an overall increase in weld performance of dissimilar joints (Scialpi et al., 2008). It was observed that by increasing the offset distance of the tool (relative to the faying surface) on the 2024 side, both the number of intercalated layers and the thickness of the layer of 2024 increase in the SZ. Hence, it can be said that the extent of material intermixing increases with the increase in tool offset distance. This was due to the increase in the tool’s contact surface area with AA 2024 at the interface, which increased the frictional heat input. Due to this, a greater volume of AA 2024 was stirred from the RS, intermixed with 6061, and deposited at the wake of the tool in the center region. In case 0.6-off (see Fig. 2c), few dark layers were observed on the AS, which means that a small amount of AA 2024 was stirred from the RS to the AS, again stipulating a greater extent of material intermixing. Moreover, this also indicates that the shoulder-driven material flow has majorly occurred, which is true for the case of FSW of thin sheets since the contribution of heat due to the tool’s shoulder-workpiece interaction is relatively more than that of the tool’s pin-workpiece interaction (Reynolds, 2008).

3.2. Tensile properties

Uniaxial tensile test was carried out to determine the different tensile properties of welded samples that were prepared perpendicular to the welding direction. A comparative bar plot was used to represent the varying yield strength (YS), ultimate tensile strength (UTS), and percentage elongation with respect to different tool offset distances (see Fig. 3). Additionally, weld efficiency (η_{weld}) was calculated, which was defined as the ratio of the UTS obtained for a particular case to the UTS of the least-strength base material (=315 MPa of AA6061). Along with the tensile properties and η_{weld} , the fracture location for each case is given in Table 1. In dissimilar material welding, the strength of the weld is mainly determined by the mechanical interlocking, which results from the

Table 1

Average values of various tensile properties and fracture location of different cases.

Cases	YS (MPa)	UTS (MPa)	% elongation	η_{weld} (%)	Fracture location
0-off	187.75	219.28	1.55	69.61	SZ
0.4-off	194.94	230.89	1.88	73.76	SZ
0.6-off	202.87	245.62	2.402	77.97	HAZ of 6061

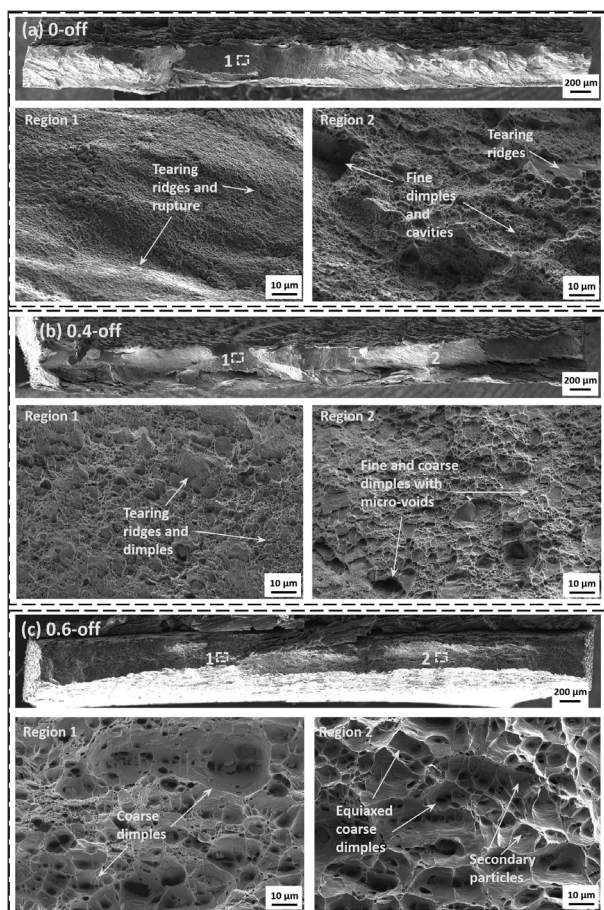


Fig. 4. Fracture morphologies of (a) 0-off, (b) 0.4-off, and (c) 0.6-off, obtained using FE-SEM with the magnified views of the selected regions.

formation of intercalated layers. The formation of the intercalated layers produces a complex fracture path when the sample is subjected to external loading, resulting in higher tensile strength (Venkateswaran & Reynolds, 2012). From the plot, it was observed that with the increase in offset distance on the 2024 side, the YS, UTS, and percentage elongation increase. This can be attributed to the increase in the number of intercalated layers or higher degree of material intermixing, eventually resulting in superior weld performance (see Fig. 2). The highest η_{weld} equal to 77.97% (UTS = 245.62 MPa) was obtained in the case of 0.6-off, in which most numbers of intercalated layers were observed. Moreover, it

can be said that in this case, the weld fractures from the HAZ of the 6061 side, which indicate that the strength of SZ was actually higher than 245.62 MPa. Whereas, in the case of 0-off and 0.4-off, the weld fractures from the SZ; hence the value obtained reflects the strength of the SZ itself in these cases.

3.3. Fractography

The fracture morphologies of the fractured tensile samples were analyzed using FE-SEM to understand the mode of fracture in different cases. The low-magnification and respective high-magnification images of the selected regions for all three cases are shown in Fig. 4. The welded samples fracture from different locations because of different degrees of material intermixing observed as a result of tool offset in different cases (mentioned in Table 1). Moreover, the fracture morphologies in different cases indicate various modes of fractures.

In the case of 0-off (see Fig. 4a), the weld fractures from the SZ and different modes of fracture were observed in various places in the low-magnification image. From this, two high-magnification images were obtained at different regions. In region 1, tearing ridges and rupture were observed, indicating a brittle mode of fracture. In region 2, very fine dimples and cavities with tearing ridges were observed at some places, indicating a small amount of ductility in this region. In the case of 0.4-off (see Fig. 4b) also, the weld fractures from the SZ, but a different fracture morphology was obtained compared to 0-off. However, after analyzing the high-magnification images of the two regions (regions 1 and 2), a similar fracture morphology was observed. Numerous fine and coarse dimples with micro-voids were observed, indicating that the specimen was relatively more deformed before fracture, which was evident from a higher elongation obtained than 0-off. Moreover, it can also be said that the presence of fine dimples indicates the presence of fine grains in the SZ (Vendra et al., 2017). In the case of 0.6-off, the weld fractures from the

HAZ of the 6061 side, which is a preferential fracture site for sound welded joints. In the HAZ, the dissolution of the primary hardening precipitate and coarsening of grains occurs as it is subjected to only thermal loading (Ahmed & Saha, 2020). In this case, similar fracture morphology was observed throughout the fracture surface (see Fig. 4c). High-magnification images of the two selected regions indicate the presence of equiaxed coarse dimples, which were formed due to microvoids coalescence at high strain during tensile loading. Large shape dimples represent higher fracture toughness of the welded joints, which was evident from higher percentage elongation (Hohenwarter & Pippan, 2012). Moreover, the presence of secondary phase particles (β -Mg₂Si) was observed at the bottom of the dimples, which can act as a nucleation site for microvoids during fracture of the tensile samples (Guo et al., 2014).

4. Conclusions

In the present work, dissimilar μ FSW of 0.5 mm thick AA 6061-T6 and ALCLAD 2024-T3 were carried out. The tool was offset on the 2024 (high-strength material) side to ensure the right amount of heat distribution since rapid heat dissipation is a major concern in the joining of thin sheets. Further, the effect of different tool offset positions on the weld characteristics, such as material intermixing and mechanical properties, was studied. The main outcomes were as below:

- Layer-wise mixing was observed in all the cases, and the extent of material intermixing was determined by – (a) the quantities of intercalated layers and (b) thickness of the layer of 2024 in the SZ.
- With the increase in tool offset distance on the 2024 side, the extent of material intermixing increases due to the increased frictional heat input on this side.
- Tensile characteristics (YS, UTS, and % elongation) increase with the increase in offset distance. Moreover, the highest weld efficiency of 77.97% was obtained at a tool offset distance of 0.6 mm on the 2024 side due to mechanical interlocking.
- Weld in case of 0-off and 0.4-off, fractures from the SZ, whereas in case of 0.6-off, the weld fractures from the HAZ of 6061 under ductile mode.

References

- Ahmed, S., & Saha, P. (2018). Development and testing of fixtures for friction stir welding of thin aluminium sheets. *Journal of Materials Processing Technology*, 252, 242-248. <https://doi.org/10.1016/j.jmatprotec.2017.09.034>
- Ahmed, S., & Saha, P. (2020). Selection of optimal process parameters and assessment of its effect in micro-friction stir welding of AA6061-T6 sheets. *International Journal of Advanced Manufacturing Technology*, 106(7-8), 3045-3061. <https://doi.org/10.1007/s00170-019-04840-6>
- Cavaliere, P., & Panella, F. (2008). Effect of tool position on the fatigue properties of dissimilar 2024-7075 sheets joined by friction stir welding. *Journal of Materials Processing Technology*, 206, 249-255. <https://doi.org/10.1016/j.jmatprotec.2007.12.036>
- Cole, E. G., Fehrenbacher, A., Duffie, N. A., & Zinn, M. R. (2014). Weld temperature effects during friction stir welding of dissimilar aluminum alloys 6061-t6 and 7075-t6. *International Journal of Advanced Manufacturing Technology*, 71, 643-652. <https://doi.org/10.1007/s00170-013-5485-9>
- Guo, J. F., Chen, H. C., Sun, C. N., Bi, G., Sun, Z., & Wei, J. (2014). Friction stir welding of dissimilar materials between AA6061 and AA7075 Al alloys effects of process parameters. *Materials and Design*, 56, 185-192. <https://doi.org/10.1016/j.matdes.2013.10.082>
- Hohenwarter, A., & Pippan, R. (2012). A comprehensive study on the damage tolerance of ultrafine-grained copper. *Materials Science and Engineering A*, 540, 89-96. <https://doi.org/10.1016/j.msea.2012.01.089>
- Jonckheere, C., De Meester, B., Denquin, A., & Simar, A. (2012). Dissimilar friction stir welding of 2014 to 6061 aluminum alloys. *Advanced Materials Research*, 409, 269-274. <https://doi.org/10.4028/www.scientific.net/AMR.409.269>
- Kumar, K., & Kailas, S. V. (2010). Positional dependence of material flow in friction stir welding: Analysis of joint line remnant and its relevance to dissimilar metal welding. *Science and Technology of Welding and Joining*, 15(4), 305-311. <https://doi.org/10.1179/136217109X12568132624280>
- Mao, Y., Ni, Y., Xiao, X., Qin, D., & Fu, L. (2020). Microstructural characterization and

mechanical properties of micro friction stir welded dissimilar Al/Cu ultra-thin sheets. *Journal of Manufacturing Processes*, 60 (October), 356-365. <https://doi.org/10.1016/j.jmapro.2020.10.064>

Reynolds, A. P. (2008). Flow visualization and simulation in FSW. *Scripta Materialia*, 58, 338-342. <https://doi.org/10.1016/j.scriptamat.2007.10.048>

Scialpi, A., De Filippis, L. A. C., Cuomo, P., & Di Summa, P. (2008). Micro friction stir welding of 2024-6082 aluminium alloys. *Welding International*, 22(1), 16-22. <https://doi.org/10.1080/09507110801936069>

Teh, N. J., Goddin, H., & Whitaker, A. (2011). *Developments in micro applications of friction stir welding*. Cambridge UK TWI Dense. <https://www.twi-global.com/technical-knowledge/published-papers/developments-in-micro-applications-of-friction-stir-welding/>.

Threadgill, P. L., Leonard, A. J., Shercliff, H. R., & Withers, P. J. (2009). Friction stir welding of aluminium alloys. *International Materials Reviews*, 54(2), 49-93. <https://doi.org/10.1179/174328009X411136>

Vendra, S. S. L., Goel, S., Kumar, N., & Jayaganthan, R. (2017). A study on fracture toughness and strain rate sensitivity of severely deformed Al 6063 alloys processed by multiaxial forging and rolling at cryogenic temperature. *Materials Science and Engineering A*, 686(January), 82-92. <https://doi.org/10.1016/j.msea.2017.01.035>

Venkateswaran, P., & Reynolds, A. P. (2012). Factors affecting the properties of Friction Stir Welds between aluminum and magnesium alloys. *Materials Science and Engineering A*, 545, 26-37. <https://doi.org/10.1016/j.msea.2012.02.069>

Verma, M., Ahmed, S., & Saha, P. (2021). Challenges, process requisites / inputs , mechanics and weld performance of dissimilar micro-friction stir welding (dissimilar μ FSW): A comprehensive review. *Journal of Manufacturing Processes*, 68(PA), 249-276. <https://doi.org/10.1016/j.jmapro.2021.05.045>



Mayank Verma is currently a doctoral research fellow in the Department of Mechanical Engineering, Indian Institute of Technology Patna (IIT-P), India. He received his master's degree (M.Tech) in Manufacturing Engineering in the year 2018 from the National Institute of Foundry and Forge Technology (NIFFT), India. He received his bachelor's degree (B.E.) in the year 2015 in Mechanical Engineering from Chhattisgarh Swami Vivekanand Technical University (CSVTU), India. His current research topic is "Dissimilar micro-friction stir welding" or "joining of ultra-thin dissimilar sheets using friction stir welding". His area of expertise is solid-state welding, material characterization, mechanical analysis, and computer-assisted numerical analysis. He has got two publications in the "Journal of Manufacturing Processes" and in the "Journal of Materials Processing Technology" along with one book chapter. (E-mail: 1821me11@iitp.ac.in)



Dr. Probir Saha is currently working as a Head and Associate Professor in the Department of Mechanical Engineering, IIT Patna. He obtained his Ph.D in 2009 from IIT Kharagpur, M.Tech from IIT Delhi in 2002, and B.E. from Jadavpur University in 2001. He has already guided three Ph.D students who have got opportunities from IIT and foreign universities in faculty and postdoctoral positions. Five more Ph.D students are presently working under his supervision. He is currently doing active research on micro-EDM, micro-EDG, and micro-FSW. His other research includes AFS-D. He is also working on several projects funded by different agencies.